ENVIRONMENTAL RESEARCH LETTERS

PURPOSE-LED PUBLISHING™

Part of the ENVIRONMENTAL RESEARCH SERIES

LETTER • OPEN ACCESS

Atmospheric patterns drive marine heatwaves in the North Atlantic and Mediterranean Sea during summer 2023

To cite this article: Lorine Behr *et al* 2025 *Environ. Res. Lett.* **20** 104020

ENVIRONMENTAL RESEARCH
LETTERS

OPEN ACCESS

RECEIVED
27 June 2025

REVISED
16 August 2025

ACCEPTED FOR PUBLICATION
28 August 2025

PUBLISHED
5 September 2025

LETTER

Atmospheric patterns drive marine heatwaves in the North Atlantic and Mediterranean Sea during summer 2023

Lorine Behr[1,*], **Elena Xoplaki**[2,3], **Niklas Luther**[1], **Simon A Josey**[4] and **Jürg Luterbacher**[1,3]

[1] Center for international Development and Environmental Research, Justus Liebig University Giessen, Giessen, Germany
[2] CMCC Foundation - Euro-Mediterranean Center on Climate Change, Bologna, Italy
[3] Department of Geography, Climatology, Climate Dynamics and Climate Change, Justus Liebig University Giessen, Giessen, Germany
[4] National Oceanography Centre, Southampton, United Kingdom
[*] Author to whom any correspondence should be addressed.

E-mail: Lorine.Behr@zeu.uni-giessen.de

Keywords: marine heatwaves, teleconnection patterns, North Atlantic, Mediterranean Sea, extreme events, RGCCA, multi-block data analysis

Supplementary material for this article is available online

Abstract

The year 2023 experienced record-breaking marine heatwaves (MHWs) across the North Atlantic and Mediterranean Sea, contributing to the highest global surface air and sea surface temperatures (SSTs) on record. These events were exceptional in intensity, persistence, and spatial extent, reflecting the combined influence of anthropogenic warming, short-term climate modes and complex atmosphere-ocean interactions. This study investigates the large-scale atmospheric drivers behind these extremes using NOAA OISST v2.1 and ERA5 reanalysis datasets. We characterize MHWs from May to August 2023, analyze surface and mid-tropospheric anomalies in pressure, air temperature, wind and air–sea heat flux and apply regularized generalized canonical correlation analysis (RGCCA) to study multivariate links between atmospheric variability and MHW characteristics. Our findings show that the Subtropical Atlantic experienced the longest MHW, the Northwest Atlantic the most intense, and the Western Mediterranean the most frequent events. The summer North Atlantic Oscillation (NAO) and Scandinavian Pattern (SCAN) emerged as key modulators of MHWs. Compound configurations of $NAO^{-}/SCAN^{+}$ in July-August and $NAO^{+}/SCAN^{-}$ in May-June generated persistent atmospheric ridges and weakened the Azores High, which in turn suppressed winds, altered heat fluxes and mixed layer depths, and promoted stratification—leading to sustained surface warming. The leading RGCCA mode explains more than 40% of the SSTA variability and shows statistically robust correlations ($r = 0.81$–0.94) between atmospheric drivers and MHW evolution. This multivariate approach demonstrates how teleconnection patterns co-modulate regional MHW dynamics, underscoring the importance of compound atmospheric influences. Our results highlight the utility of RGCCA in diagnosing complex climate extremes and support the integration of large-scale atmospheric indicators into early warning systems and adaptation planning in the face of increased marine heat stress.

1. Introduction

Marine heatwaves (MHWs) are extreme, prolonged periods of high sea surface temperature anomalies (SSTAs) that have gained increasing attention due to their significant ecological, socioeconomic and climatic impacts. These events, defined by the occurrence of SSTA that persist over a prolonged period (Hobday *et al* 2016), can severely impact marine ecosystems, leading to habitat shifts (Mills *et al* 2013), alterations in population structure (Hughes *et al* 2018, Cheung and Frölicher 2020) and widespread mortality among a range of marine species (Garrabou *et al* 2009, 2022, Smale *et al* 2019, Wernberg *et al* 2021, Smith *et al* 2023). The IPCC Sixth Assessment Report (2022) concluded with high confidence that MHWs have doubled in frequency since the 1980s and are now more intense, longer-lasting, and more widespread—trends very likely attributable to human influence (Capotondi *et al* 2024, Marcos *et al* 2025). While the long-term trend of global ocean warming is widely recognized as a primary driver of MHWs, it fails to account for the short-term or interannual variability that shapes MHW occurrence and severity (Frölicher *et al* 2018, Schlegel *et al* 2021, Simon *et al* 2023a).

Recent studies have emphasized that MHWs are also influenced by a complex interplay of local and remote atmospheric processes that operate across various spatial and temporal scales (Holbrook *et al* 2019, Sen Gupta *et al* 2020, Schlegel *et al* 2021). Key drivers of MHW variability include large-scale atmospheric and oceanic patterns that modulate air-sea heat fluxes (ASHFs), wind patterns and mixed layer depth (MLD, Schlegel *et al* 2021, Vogt *et al* 2022). These processes play a crucial role in shaping the spatial and temporal patterns of SSTA and contribute to the variability observed in MHWs across different oceanic regions, including the Mediterranean Sea (MedSea; e.g. Bensoussan *et al* 2019, Ibrahim *et al* 2021, Androulidakis and Krestenitis 2022, Hamdeno and Alvera-Azcaráte 2023, Pastor and Khodayar 2023, Simon *et al* 2023a), the Northwest Atlantic (NWAtlantic; Chen *et al* 2014, Filbee-Dexter *et al* 2020, Perez *et al* 2021, Schlegel *et al* 2021, Sims *et al* 2022), and the Northeast Atlantic (NEAtlantic; McCarthy *et al* 2023, Simon *et al* 2023b, Berthou *et al* 2024, Dong *et al* 2025, England *et al* 2025).

In the North Atlantic (NAtlantic)–Mediterranean region, atmospheric circulation strongly influences marine extremes, with interannual variability dominated by the North Atlantic Oscillation (NAO)—a large-scale pressure pattern between the Azores and Iceland (Hurrell *et al* 2003). Although the NAO represents the dominant mode of variability in this region, atmospheric circulation is also modulated by other teleconnection patterns, notably the Scandinavian Pattern (SCAN, Bueh and Nakamura 2007) and East Atlantic Pattern (EAP, Barnston and Livezey 1987). These patterns involve pressure anomalies over different parts of the NAtlantic and Europe, modifying local SSTs by altering wind patterns and ASHF and contributing to the occurrence of atmospheric and MHWs (Josey *et al* 2011, Chafik *et al* 2017, Hamdeno and Alvera-Azcaráte 2023, Simon *et al* 2023a).

The need to better understand MHWs and their atmospheric drivers became particularly evident in 2023, a year that broke global surface temperature records and experienced an unprecedented frequency of extreme temperature days and MHW events (Capotondi *et al* 2024, England *et al* 2025, supplementary figure 1(a)). These events were linked to the combined effects of the Atlantic Multidecadal Oscillation, El Niño and rising greenhouse gas concentrations (Blunden and Boyer 2024, Li *et al* 2024). Terhaar *et al* (2025) report that this jump in global SSTs—exceeding the previous record by at least 0.25 °C—is an event expected only once every 512 years under the current long-term warming trend. Notably, 2023 saw intense MHWs that affected large portions of the NAtlantic and Mediterranean, with the Subtropical Atlantic (SubTAtlantic) and NWAtlantic experiencing exceptionally high temperatures starting as early as March 2023 (Kuhlbrodt *et al* 2024, Dong *et al* 2025). This warming led to the most extensive coral bleaching event ever recorded in the Northern Hemisphere (Goreau and Hayes 2024), highlighting the critical need to better understand the atmospheric drivers behind these unprecedented extreme events. Despite the increasing occurrence and impact of MHWs, comprehensive analyses of the 2023 NAtlantic and MedSea MHWs and their atmospheric drivers are limited. Studies have reported SSTA to illustrate the severity of these events, though often without applying a consistent, threshold-based definition of MHWs. For example, Marullo *et al* (2023) identified the 2022–2023 Mediterranean MHW as the longest in four decades (from January 2022-April 2023) based on SSTA without defining the MHW, introducing uncertainty regarding the event's true extent. Similarly, studies by Kuhlbrodt *et al* (2024) and England *et al* (2025) as well as McCarthy *et al* (2023) and Berthou *et al* (2024) have analyzed the severity of SSTA and the MHW in the NAtlantic, respectively, without exploring the relationship between these events and large-scale atmospheric modes. Nevertheless, they consistently agree that the NAtlantic MHW was mainly driven by atmospheric processes—particularly weak surface winds that led to shallower mixed layers and increased ASHF. Furthermore, Dong *et al* (2025) and England *et al* (2025) found that reduced latent and sensible heat loss, along with enhanced solar radiation, were the dominant drivers of the extreme warming, while oceanic heat advection played a minor role.

Here, we address this gap concerning large-scale atmospheric modes by investigating May–August (MJJA) 2023 MHWs using regularized generalized canonical correlation analysis (RGCCA; Tenenhaus and Tenenhaus 2011), a multivariate method well-suited to disentangle complex atmosphere-ocean interactions and identify key drivers of MHW dynamics. Focusing on short-term ocean-atmosphere dynamics, we limit this study to surface MHWs, though we acknowledge the importance of subsurface MHWs due to their persistence and potential impacts on fisheries, ecosystems as well as deep convection and overflow water formation (Behr *et al* 2022, Josey and Schroeder 2023, Le Grix *et al* 2025).

This paper is structured as follows: section 2 presents datasets and the methodology, including a detailed description of the RGCCA approach. Section 3 outlines the characteristics and categorization of MHWs at key locations in the NAtlantic and MedSea during MJJA 2023. Section 4 analyses the atmospheric circulation during two key MHW periods in May-June and July-August 2023, focusing on both surface and mid-tropospheric conditions. Section 5 presents the results of the RGCCA analysis, identifying the dominant atmospheric modes of variability associated with MHWs and discussing their relevance for improving our understanding and prediction of future MHW events.

2. Data and methods

2.1. NOAA OI SST and ERA5 datasets

To detect MHWs and analyze their characteristics, we use the daily gridded National Oceanic and Atmospheric Administration Optimum Interpolation SST version 2.1 dataset (NOAA OISST v2.1, Huang *et al* 2021, updated), which covers the NAtlantic and MedSea regions (90° W–40° E, 10° – 80° N). This dataset, derived from the Advanced Very High-Resolution Radiometer satellite, *in-situ* ship, and buoy observations, provides daily data from 1982 to the present.

In addition to SSTs, we analyze key meteorological variables to investigate atmosphere–ocean interactions: Surface and mid-tropospheric circulation are represented by anomalies in sea level pressure (SLPA) and 500 hPa geopotential height (zg_{500}A), which influence 2 meter maximum temperature anomalies (T_{max}A)—an estimate for the atmospheric thermal state. T_{max}A affect SSTs and modulate near-surface wind anomalies (U_{10}A and V_{10}A), which in turn influence ASHF anomalies, including latent (Q_{LH}A) and sensible (Q_{SH}A) heat fluxes as well as net shortwave (Q_{SW}A) and net longwave radiation (Q_{LW}A). These processes collectively shape the duration and intensity of MHWs.

All meteorological variables were obtained from the European Centre for Medium-Range Weather Forecasts ERA5 reanalysis (Hersbach *et al* 2020, updated). We compute daily wind speed anomalies (windA) from U_{10}A and V_{10}A, and the net ASHF anomalies (Q_{net}A) as the sum of the four ASHF variables. We use ERA5 and NOAA OISST datasets to ensure consistency and to facilitate comparison with most MHW studies. Both datasets are provided on a high-resolution 1/4° latitude-longitude grid. Since the grid cells are staggered by 1/8° in the NOAA product, we performed bilinear interpolation to align it with the ERA5 grid. We analyze daily SSTA and meteorological data anomalies from MJJA 2023, with anomalies calculated relative to the 30 year reference period 1983–2012 to allow comparison with existing MHW papers (Hobday *et al* 2018).

2.2. MHW detection

To detect MHWs, we employed the widely adopted approach of Hobday *et al* (2016). MHWs are defined as periods during which SSTA exceed the seasonally-varying 90th percentile threshold, relative to the local 30 year baseline climatology (1983–2012), for at least five consecutive days. Events interrupted by fewer than two days are considered as a single continuous event. The severity of MHWs is categorized using a four-step scheme, ranging from 'moderate' to 'extreme', based on the first to four times 90th percentile thresholds (Hobday *et al* 2018). Category IV means, for example, that the SSTA values exceed the difference between the mean and the 90th percentile threshold by a factor of four. After identifying MHW events, we calculated the mean and maximum intensity, mean duration, frequency and cumulative mean intensity (time-integrated temperature anomaly over each event duration) from MJJA 2023.

2.3. RGCCA

Canonical correlation analysis (CCA) is a statistical method used to identify relationships between two datasets by finding linear combinations of variables that maximize their correlation. While effective in many applications, traditional CCA has limitations when applied to high-dimensional datasets such as those found in climate science (Xoplaki *et al* 2003a, 2003b). For instance, CCA assumes the absence of collinearity among input variables, a condition rarely met in climate datasets due to inherent spatial correlations. Consequently, it has become standard practice, following the work of Barnett and Preisendorfer (1987), to apply principal component analysis (PCA) beforehand to extract uncorrelated components from the spatially correlated data prior to conducting CCA.

RGCCA extends CCA by incorporating multiple interdependent datasets (blocks) and adding regularization techniques that prevent multicollinearity, overfitting and improve stability also when working with noisy, high-dimensional or incomplete datasets. These enhancements make RGCCA a powerful tool for climate data analysis, where multiple interrelated variables are the norm and their joint use can improve the physical interpretability and robustness of the results. Thus, RGCCA enables a more comprehensive analysis of climate teleconnections, enhancing the identification of significant patterns of climate variability. The method has been extensively developed in the statistical literature and has been applied in various scientific fields, including genomics and neuroscience (e.g. Tenenhaus and Tenenhaus 2011, Tenenhaus *et al* 2017, Garali *et al* 2018).

In our study, we consider $J \in N$ climate variables, which are organized into a matrix format similar to PCA, yielding blocks $X_1, X_2, \ldots, X_J \in R^{p \times t}$, where $p \in N$ denotes the number of grid points and $t \in N$ the number of time points. The target variable is represented by X_J. We use SSTA covering the SubTAtlantic, NEAtlantic and MedSea region (25° W–40° E, 20° N–55° N) as our response variable (X_J) and SLPA, zg_{500}A, T_{max}A, windA and Q_{net}A from a broader NAtlantic/MedSea area (90° W–40° E, 10° –80° N) as our set of predictors (X_1, .. X_{J-1}). In the following, we apply RGCCA using the Horst scheme, estimate the regularization parameters using the analytical approach of Schäfer and Strimmer (2005) and connect the blocks following the framework of Generalized CCA (Carroll 1968a, 1968b). Furthermore, to include spatial information, we use the weighting scheme of North *et al* (1982). For further details on the methodology, the reader is referred to Tenenhaus and Tenenhaus (2011) and supplementary section 1.

3. MHW characteristics

From MJJA 2023, almost the entire NAtlantic and MedSea recorded at least one MHW (figures 1 and 2(a)). Examining the extended summer season of 2023, several MHW hotspots were identified. SSTA time series from eight locations highlight the 90th percentile thresholds of MHW categories, providing local and temporal insights (figure 1). The most intense MHWs were recorded in the NWAtlantic and Western Mediterranean Sea (WMed, table 1, figure 1), areas characterized by high SSTA variability (supplementary figure 1(b)). The MHW category 'severe' was observed in the NEAtlantic, NEAtlantic, Alboran Sea (AlbSea), and Eastern Mediterranean Sea (EMed; figure 1; Hobday *et al* 2018).

Temporal patterns differed across regions: the NEAtlantic and WMed experienced MHWs primarily in May and June, while the NWAtlantic and EMed recorded MHWs from mid-July to early August, with a brief interruption before continuing until the

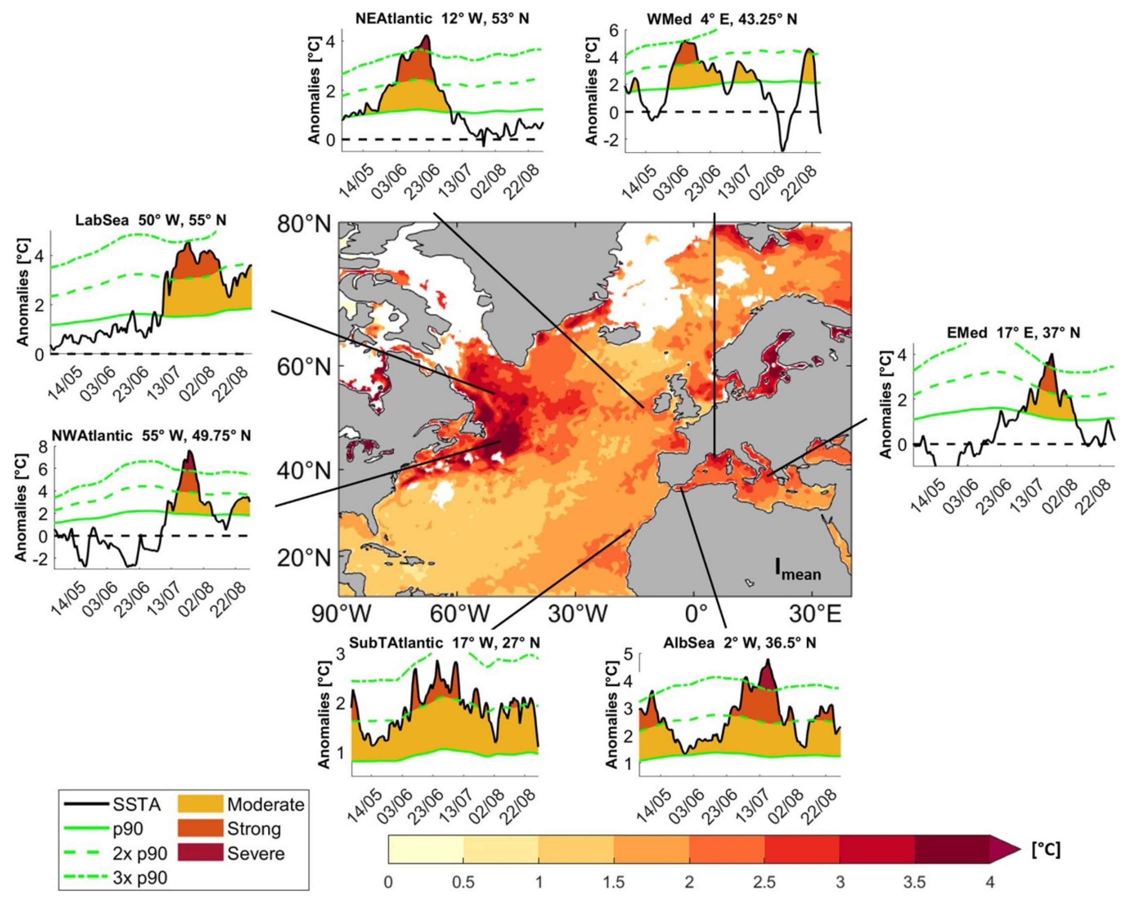

Figure 1. Mean marine heatwave (MHW) intensity from May to August 2023 (in °C): spatial map of MHW intensity across the North Atlantic and the Mediterranean Sea along with time series of the daily mean sea surface temperature anomalies for various locations. The time series indicate MHW categories ranging from moderate to severe, based on the 90th percentile thresholds defined by Hobday *et al* (2018). Abbreviations: NEAtlantic is Northeast Atlantic, LabSea is Labrador Sea, NWAtlantic is Northwest Atlantic, SubTAtlantic is Subtropical Atlantic, AlbSea is Alboran Sea, EMed is Eastern Mediterranean Sea and WMed is Western Mediterranean Sea.

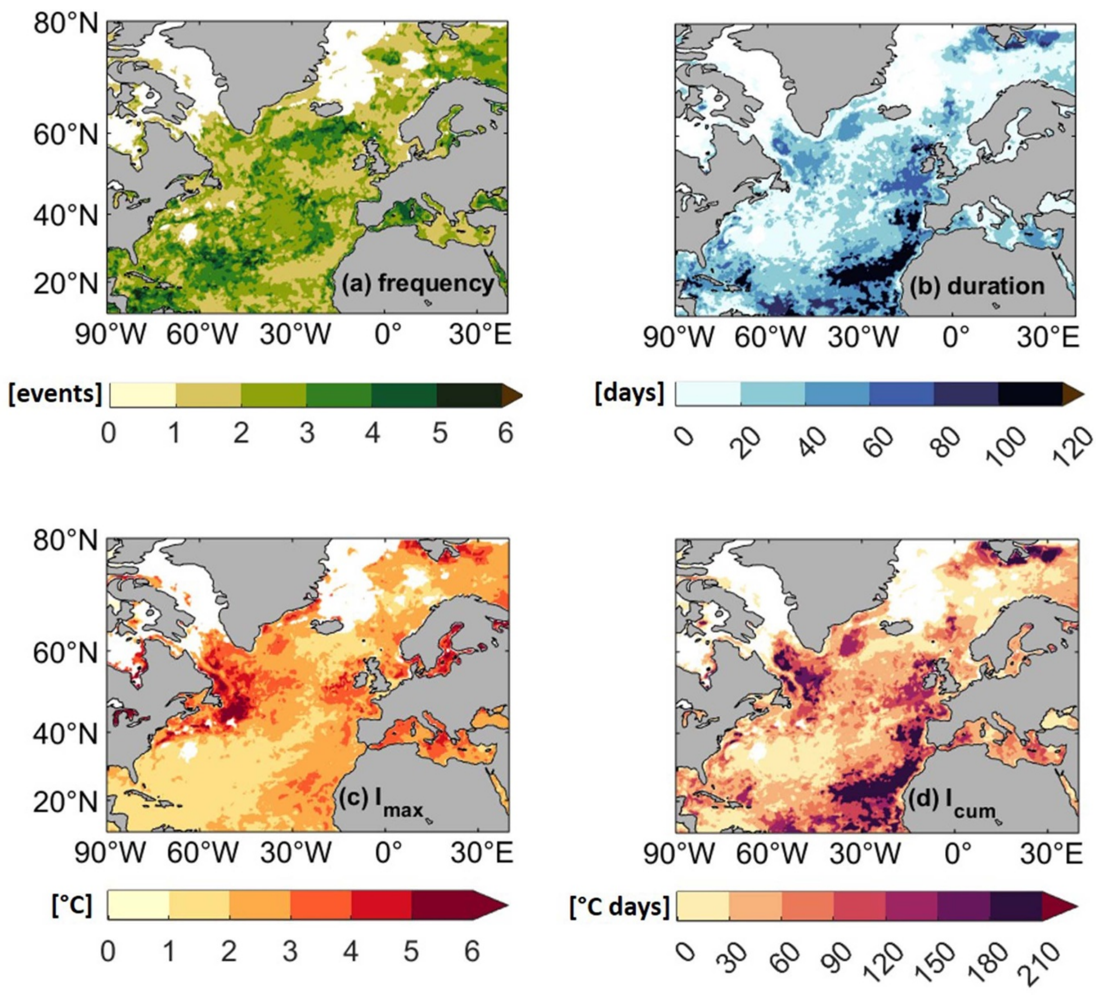

Figure 2. May to August 2023 marine heatwave characteristics of the study area: (a) marine heatwave frequency/number of events, (b) mean duration in days, (c) maximum intensity in °C, (d) cumulative intensity in °C days.

Table 1. Marine heatwave characteristics at various locations averaged over May to August 2023: marine heatwave Location, I_{mean} and I_{max} are mean and maximum intensity in °C, F_{2023} is frequency of events/number of events, D_{mean} is (mean) duration in days, I_{cum} is cumulative intensity in °C days. We used the same locations as in figure 1.

Location	I_{mean} (°C)	I_{max} (°C)	F_{2023} (events)	D_{mean} (days)	I_{cum} (°C days)
NEAtlantic	2.5	4.2	1	35	132
NWAtlantic	4.0	5.5	2	20	82
LabSea	3.5	4.5	1	55	193
SubTAtlantic	1.9	2.9	1	123	230
AlbSea	2.7	4.8	1	123	327
WMed	3.5	4.0	4	17	58
EMed	2.4	4.0	1	34	81

end of the month (figure 1). In contrast, MHWs in the SubTAtlantic and AlbSea lasted throughout the entire summer, demonstrating notable regional persistence.

Significant variability was observed in MHW metrics across these regions. The Labrador Sea (LabSea), the SubTAtlantic, and the AlbSea exhibited the longest MHW durations and the highest cumulative intensities (figure 2, table 1). For context, the 1982–2020 average annual cumulative intensity in the LabSea and SubTAtlantic/AlbSea is approximately 70 °C days and 10 °C days, respectively (Chauhan *et al* 2023). By comparison, the WMed and the NWAtlantic recorded more than one MHW, albeit of shorter durations and lower cumulative intensities (figure 2, table 1).

Overall, the longest-lasting MHWs were observed in the SubTAtlantic and AlbSea, while the highest frequency occurred in the WMed. The AlbSea also experienced the highest cumulative MHW intensity (table 1). No MHWs were detected in the polar seas or in smaller areas of the NWAtlantic (figure 2(a)), emphasizing the strong spatial heterogeneity of the 2023 MHWs.

4. Atmospheric circulation: surface and mid-troposphere analysis

MHWs in 2023 impacted nearly the entire NAtlantic and MedSea, with notable regional variability in frequency, duration, and intensity. Major hotspots for severe MHWs were identified, particularly in the NWAtlantic/LabSea, NEAtlantic, SubTAtlantic and MedSea. In this section, we analyze the spatio-temporal atmospheric circulation over these affected regions and clarify how local atmospheric variables (SLP, zg_{500}, T_{max}, wind and ASHF) influenced SST and MHW evolution.

During May-June 2023, the NAtlantic experienced a high-pressure monopole, characterized by anomalous anticyclonic conditions over the NEAtlantic extending as far as the Gulf of Lions in the WMed and a weakened Azores High over the SubTAtlantic (figures 3(d) and (e) and supplementary figures 2(a) and (b)). Persistent anticyclonic conditions since fall 2022 allowed warm SSTs to re-emerge in the northwestern MedSea and AlbSea (Marullo *et al* 2023). As shown in figures 2 and 4(a)–(d), the MHW onset coincided with these regional pressure changes and a 3 °C–4 °C SST increase. SSTA peaked in mid-June, after which a low-pressure system over the NEAtlantic and Scandinavia in July disrupted the continuation of the strong to severe MHWs (figures 4(a) and (b)), setting the stage for more intense events later in the season.

In July-August 2023, the circulation was dominated by two strong atmospheric ridges: one centered over the LabSea, extending southward to the Grand Banks, and the other over the Strait of Gibraltar, most apparent in the mid-troposphere (figures 5(d) and (e) and supplementary figures 2(c) and (d))). Over the LabSea, the circulation induced a meridional jet stream shift, advecting warm air northward and initiating MHWs via increased ASHF (figure 5, Chen *et al* 2014, Schlegel *et al* 2021, Sims *et al* 2022). The anticyclone reached its peak intensity in mid-July aligned with the occurrence of highest positive SSTA in the NWAtlantic of up to +8 °C (figure 1). Following the dissipation of the positive pressure anomaly in August 2023, the category II MHW weakened but persisted through the end of the month and into September (figures 2 and 4(a)).

Simultaneously, in the MedSea, the high-pressure system extended eastward, covering the entire region by mid-July 2023 (figure 4(i)). This expansion coincided with a continuous SST increase, with the category II to III MHW peaking in mid to late July 2023 (figure 4(h)). The position of the anticyclone—and consequently the strength of the pressure gradient—strongly influenced wind speed and ASHF dynamics, leading to multiple phases of intensification and weakening throughout the period (figures 4(j) and (k)). This is consistent with Bonino *et al* (2025), who identified subtropical ridges and weakened prevailing winds as the primary synoptic drivers of Mediterranean MHWs.

The 2023 MHWs were primarily initiated by persistent anomalies in atmospheric pressure, including both strong and weakened high-pressure systems. As a causal chain, the resulting low-pressure gradient led to reduced wind speeds which in turn

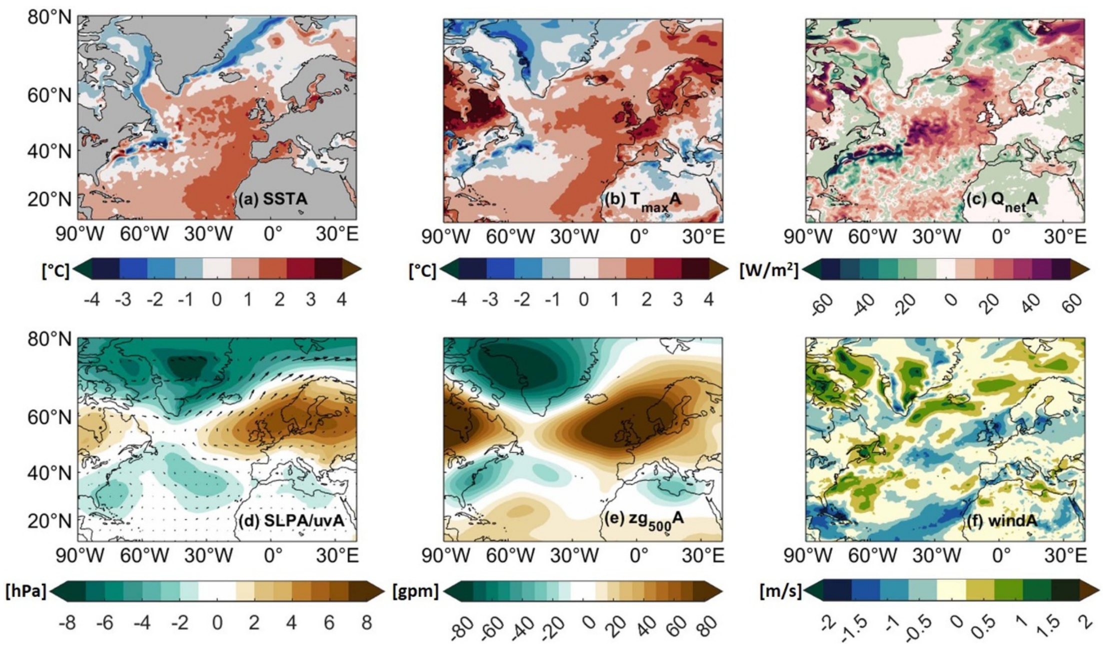

Figure 3. Mean anomalies of sea surface temperature and atmospheric variables during May–June 2023 over the North Atlantic and the Mediterranean Sea, relative to the 1983–2012 reference period: (a) sea surface temperature, (b) maximum air temperature, (c) net air-sea heat flux, (d) sea level pressure (arrows show the anomalies of the mean wind direction, (e) 500 hPa geopotential height, (f) wind speed.

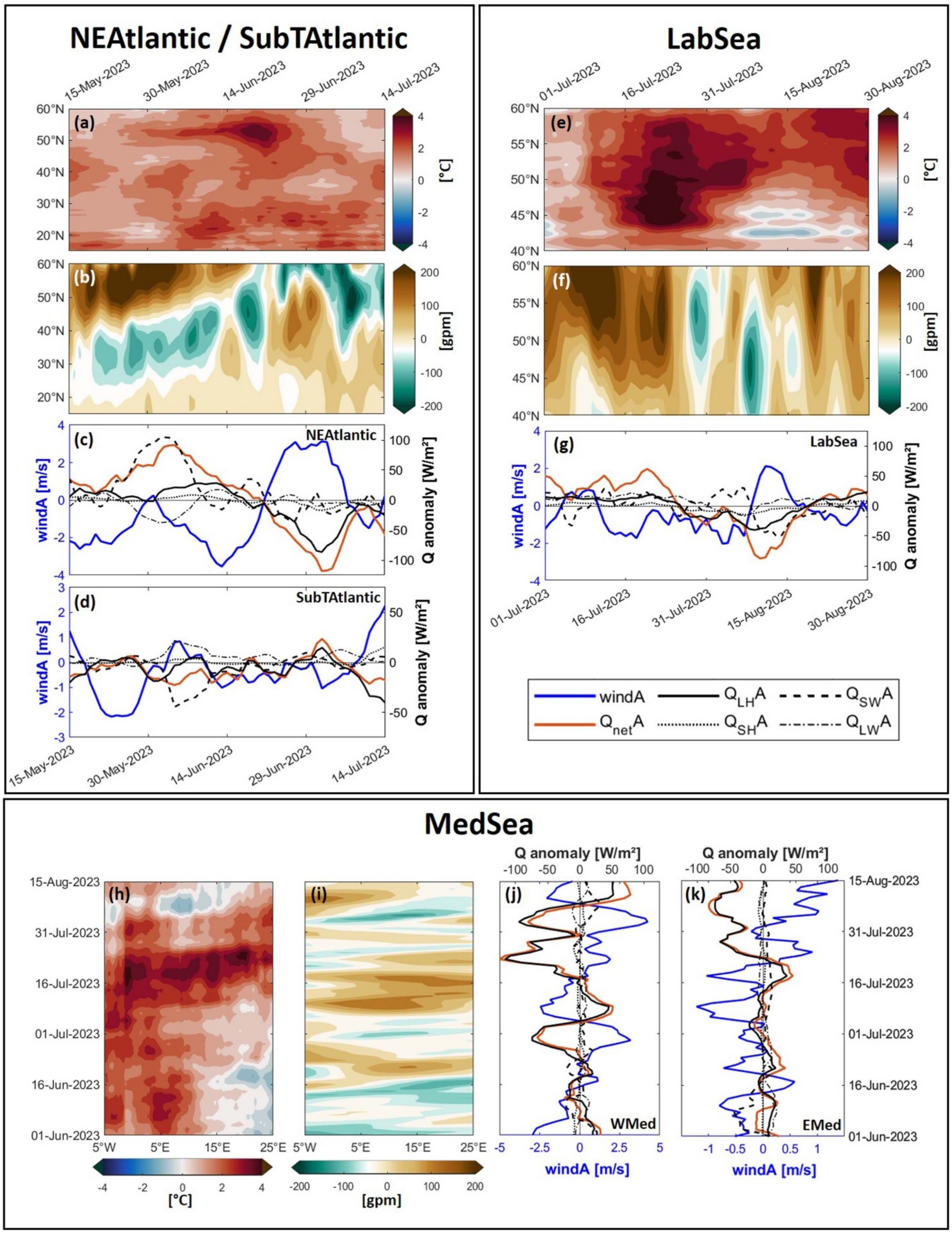

Figure 4. Temporal evolution of the May to August 2023 marine heatwaves over various subregions: (a)–(d) Northeast Atlantic and Subtropical Atlantic time-latitude Hovmoeller diagrams from 15 May to 15 July and from 15° to 60° N of (a) sea surface temperature anomalies and (b) 500 hPa geopotential height anomalies, averaged over 20° W to 10° W: (c) wind speed anomaly (blue), net air-sea heat flux anomaly (orange), anomalies of latent and sensible heat flux as well as anomalies of net shortwave and net longwave radiation (black) time series of the Northeast Atlantic (53° N, 12° W) and (d) the Subtropical Atlantic (27° N, 17° W); (e)–(g) same as (a)–(d) for the Northwest Atlantic from 1 July to 31 August: (e) + (f) same as (a) + (b) from 40° to 60° N, averaged over 55° to 40° W, (g) same as (c) for the Labrador Sea (55° N, 50° W); (h)–(k) same as (a)–(d) for the Mediterranean Sea from 1 June to 15 August: (h) + (i) same as (a) + (b) from 5° W to 25° E, averaged over 35° N to 45° N: (j) + (k) same as (c) for (j) the Alboran Sea (36.5° N, 2° W) and (k) for the Eastern Mediterranean (37° N, 17° E); reference period 1983–2012.

decreased vertical mixing and Q_{LH} and caused shoaling of the MLD (figures 3–5). Clear skies and reduced cloud cover suppressed latent and sensible heat losses, while increasing Q_{SW} resulted in an overall increase in Q_{net} and T_{max}. The rise and peak of SSTs was mostly reached after a lag (hours or days), depending on the MLD and oceanic conditions. Since the NAtlantic faced the shallowest

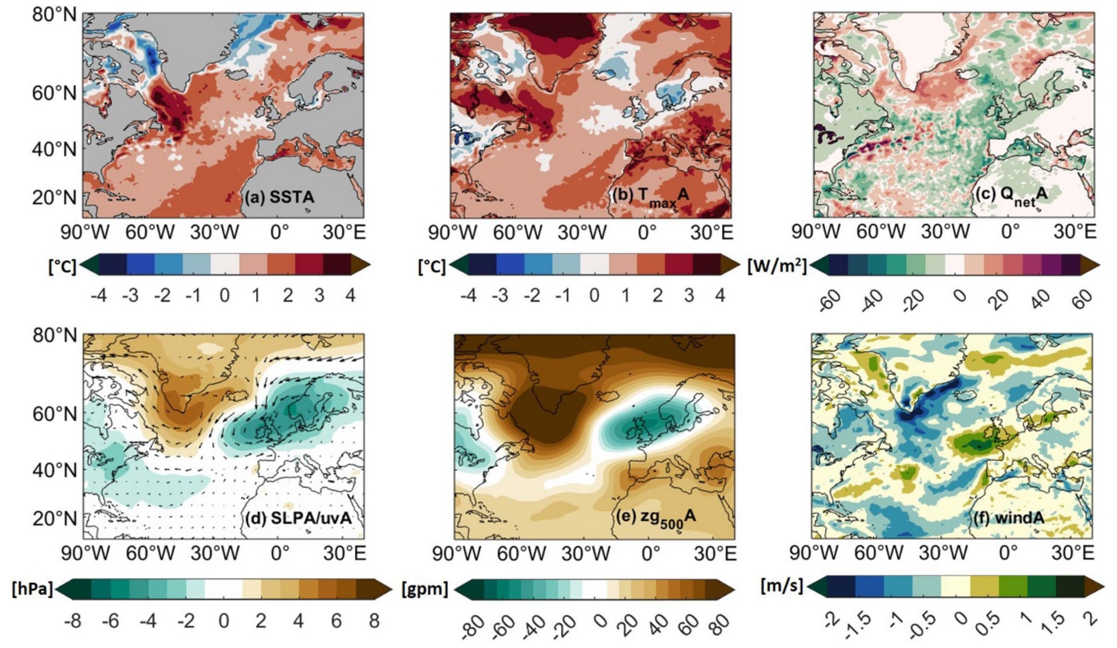

Figure 5. Same as figure 3 for July–August.

ever recorded MLD during June-July 2023 (4σ shallower than the 1981–2010 average, England *et al* 2025), SSTs rose fast and intensely especially across the NEAtlantic and NWAtlantic/LabSea (figures 4(a) and (d)).

ASHF contributions to MHWs varied regionally: in the NEAtlantic Q_{SW} dominated with anomalies over +100 W m^{-2} (figure 4(c)); in the LabSea, both Q_{SW} and Q_{LH} prevailed due to clear skies and reduced latent heat loss (figure 4(g)). In the MedSea, Q_{LH} was nearly equivalent to Q_{net} (figures 4(j) and (k)), while in the SubTAtlantic atmospheric circulation initiated the MHW, but wind-driven dynamic processes dominated, with ASHF playing a secondary role (figure 4(d)). Here, the MHW was linked to an anomalous poleward Canary Current driven by weak trade winds (20%–30% below the long-term June average, CMEMS 2023). This resulted in suppressed upwelling, stratification of the mixed layer and inhibited vertical mixing, allowing surface waters to rise and store heat more effectively.

As oceanic temperature advection played only a minor role in the MHW 2023, we do not address this further. Nevertheless, boundary currents such as the Canary Current or Gulf Stream are important distributors of heat and modulate SSTA in response to remote atmospheric forcing. Additionally, reduced Saharan dust advection and SO_2 emissions from shipping have been linked to increased SSTA due to their influence on solar radiation (Diamond *et al* 2023, Kuhlbrodt *et al* 2024, England *et al* 2025).

5. Drivers of the 2023 MHWs

From May to August 2023, MHWs across the Mediterranean-Atlantic domain were associated with anomalous pressure patterns (figures 3–5). In this section, we computed the two leading RGCCA modes for MJJA 2023 to analyze the co-variability between SSTA (25° W–40° E, 20° N–55° N) and combined large-scale atmospheric circulation patterns (90° W–40° E, 10°–80° N; SLPA, zg_{500}A, T_{max}A, Q_{net}A, windA). We also applied RGCCA over a separate domain in the NWAtlantic (80°–30° W, 35°–60° N) and obtained nearly identical results, confirming the robustness of the findings to the choice of domain (not discussed further). The first mode, which best represents the 2023 MHWs, is analyzed below; the second is shown in supplementary figure 3 and supplementary section 2.

The leading mode (figure 6) explains 40.4% of the MJJA SSTA variability in the NEAtlantic and MedSea, with correlations of the canonical variates and predictand variable SST between 0.81 and 0.94. SLPA and zg_{500}A mean conditions during May–June 2023 (figure 3) resemble the negative phase of RGCCA1, July–August 2023 (figure 5) resembles the positive phase. During RGCCA1^{+}, surface and mid-tropospheric pressure patterns form a tripole of negative anomalies over the North Sea, Great Britain, and eastern Canada, with positive anomalies over the central Mediterranean and NWAtlantic (figures 6(d) and (e)); additionally, positive SLPA are found over the Azores. RGCCA1^{-} shows the opposite. T_{max}A and Q_{net}A indicate warm (cool) conditions

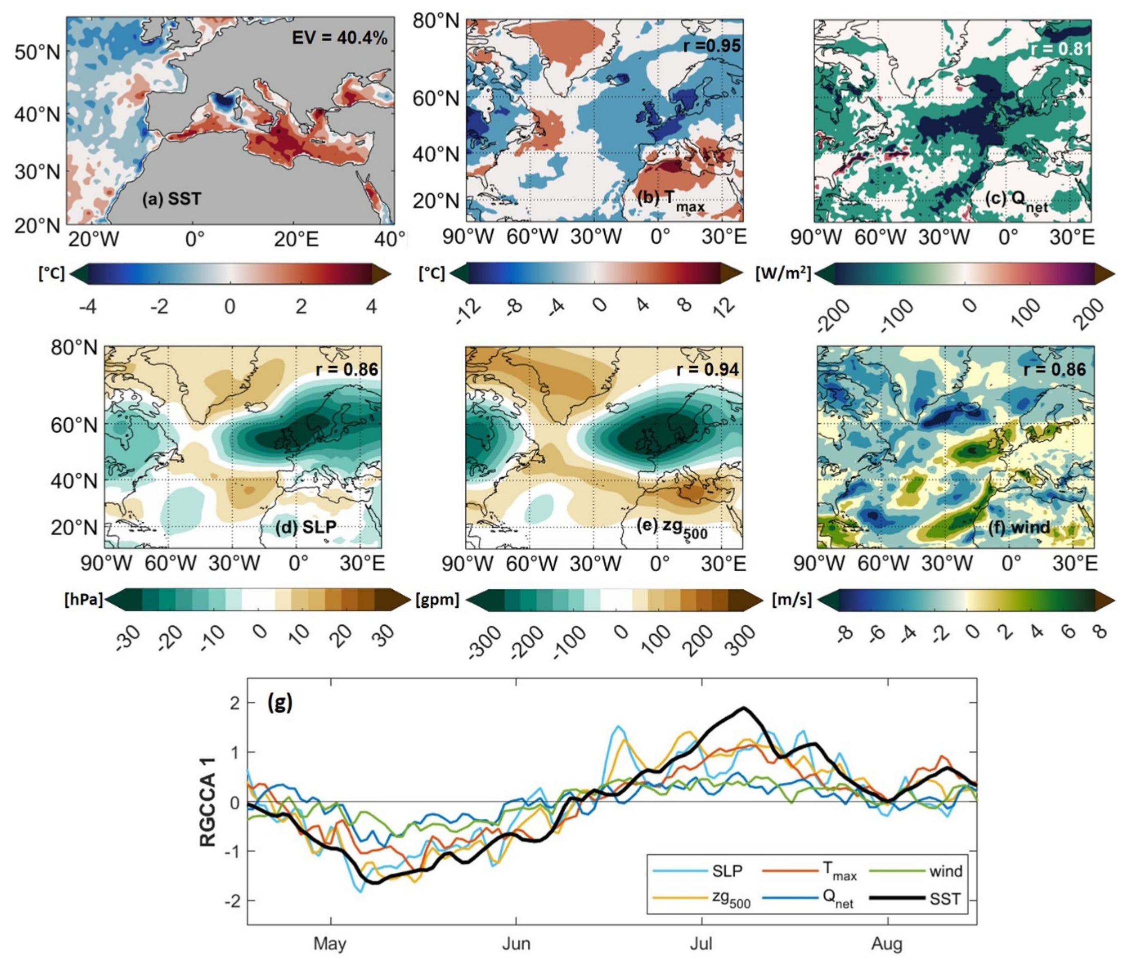

Figure 6. Patterns of the first RGCCA of (a) the Northeast Atlantic/Subtropical Atlantic/Mediterranean Sea field of the sea surface temperature response variable and each of the five predictor fields (b) maximum air temperature, (c) net air–sea heat flux, (d) sea level pressure, (e) geopotential height at 500 hPa, (f) wind speed, (g) normalized time components of RGCCA1; the explained variance (EV) of SST and correlation coefficients (r) of the time components of the predictors and SST are shown in the top right corners of the patterns.

with increased (decreased) heat uptake, while windA shows reduced (enhanced) wind speeds (figure 6). SSTA is warmer (cooler) across most of the MedSea, except the Gulf of Lions where the reverse appears (figure 6(a)).

These spatial patterns are supported by daily RGCCA components (figure 6(g)): They capture positive (negative) SSTA events accumulated in July-early August (May–June), consistent with the observed 2023 MHWs (figures 2–5 and 6(g)). The mid-tropospheric pressure anomalies in RGCCA1$^+$ (RGCCA1$^-$) resemble the negative (positive) phase of the summer NAO ($r = -0.62$; 5% significance level) and the positive (negative) phase of the summer SCAN ($r = 0.41$; figure 7; Barnston and Livezey 1987, Hurrell *et al* 2003, Cassou *et al* 2005, Bueh and Nakamura 2007, Folland *et al* 2009, Simon *et al* 2023a, figure 7). RGCCA1$^+$ (RGCCA1$^-$) also matches the North Sea cluster negative (positive) phase (Stefanon *et al* 2012). In general, the interaction between the NAO and SCAN leads to clockwise (anticlockwise) shifts in the centers of action when the two patterns share the same (opposite) phase (see Chafik *et al* 2017).

Building on this framework, we find that the Euro-Atlantic circulation underwent a pronounced transition over the summer of 2023. The early summer was characterized by a NAO$^+$ pattern with low pressure over Greenland and the LabSea and high pressure over the NEAtlantic (May–June category III MHW). By July–August, the circulation shifted to a pronounced NAO$^-$ regime with a blocking high over the LabSea (July-August category II MHW, figure 6+7). Our findings align with Holbrook *et al* (2019), who report >40% more MHW days in the NWAtlantic during NAO$^-$ phases. Strong EAP$^-$ conditions may have contributed to the persistent blocking over the NEAtlantic (figure 7(e)). Simultaneously, Scandinavia shifted from a ridge (SCAN$^-$) to a sustained trough (SCAN$^+$), while downstream ridging intensified over the MedSea (category II–III MHW).

Finally, the drivers behind this regime shift (RGCCA$^-$ to RGCCA$^+$) likely reflect a combination of oceanic and atmospheric influences.

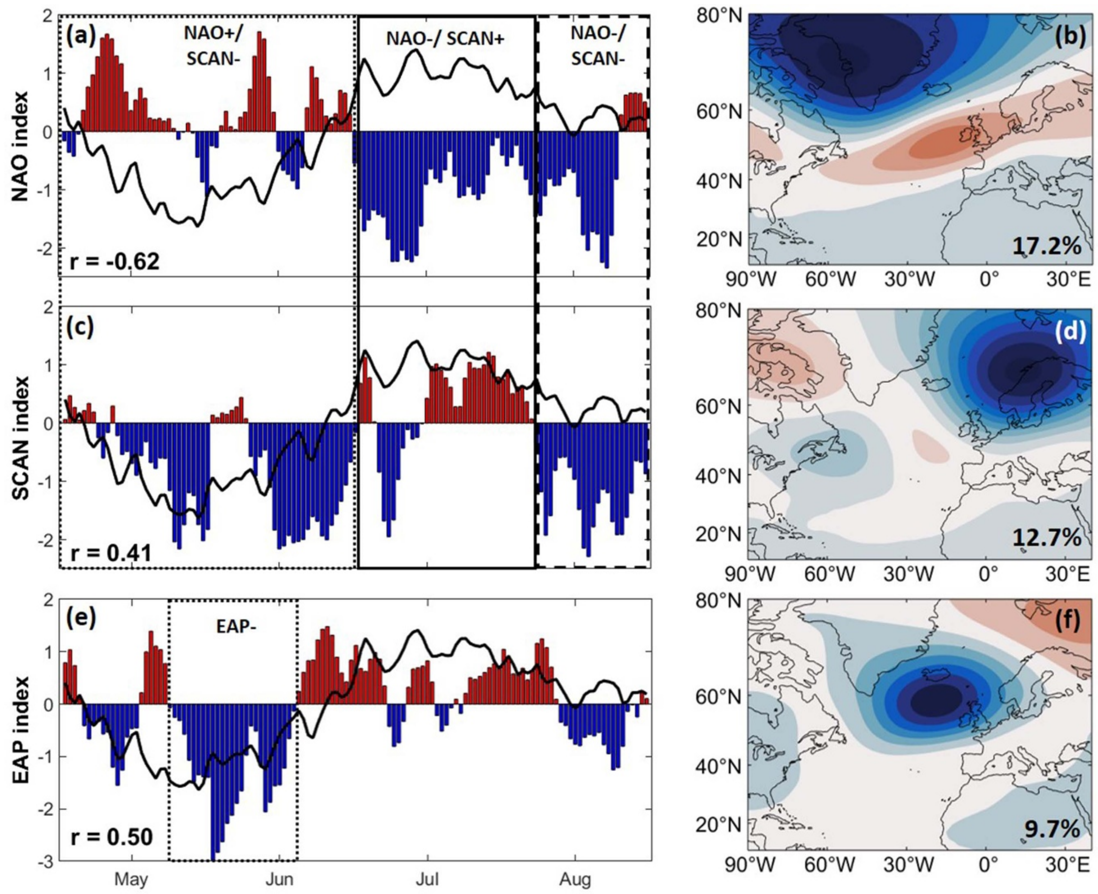

Figure 7. (a)/(c)/(e) Daily North Atlantic Oscillation (NAO)/Scandinavian Pattern (SCAN)/East Atlantic Pattern (EAP) indices (bars) and 500 hPa geopotential height anomaly time component of the first mode regularized generalized canonical correlation analysis (RGCCA1; black line) from May to August 2023; the Pearson's correlation coefficient between the NAO and first mode is −0.6, between the SCAN and the first mode is 0.4 and between the EAP and the first mode is 0.5, significant on the 95% confidence level, the dotted black line shows a period of NAO^+, $SCAN^-$ and EAP^-, the solid black line shows a period of NAO^- and $SCAN^+$, and the dashed black line shows a period of NAO^- and $SCAN^-$; (b)/(d)/(f) First/second/third empirical orthogonal function of the summer (June–July–August) long-term mean 500 hPa geopotential height anomaly explaining 17.2%, 12.7% and 9.7% of the total variance, respectively.

Anomalously warm western SubTAtlantic SSTs favor enhanced subtropical ridging and NWAtlantic blocking (e.g. Rodríguez-Fonseca *et al* (2015), O'Reilly *et al* (2017)), while land-atmosphere feedbacks over eastern Europe and western Russia amplify stationary Rossby waves, promoting continental blocking (e.g. Miralles *et al* (2014); Kornhuber *et al* (2017). Together, these drivers facilitated a more meridional jet stream configuration, enhancing the persistence of heat extremes over the MedSea and wetter conditions over Scandinavia.

6. Conclusion

The summer of 2023 witnessed some of the most intense and persistent MHWs ever recorded in the NAtlantic and MedSea, coinciding with record-breaking global surface air and ocean temperatures. Using high-resolution NOAA OISST and ERA5 reanalysis data, this study provides a detailed diagnosis of the spatial and temporal characteristics of MHWs from May to August 2023 and offers a novel multivariate attribution of their atmospheric drivers using RGCCA. Our results show that the extreme surface warming was not solely a consequence of long-term ocean trends but was strongly modulated by short-term atmospheric variability. In particular, the co-evolution of NAO^- and $SCAN^+$ during July-August was critical in sustaining and amplifying MHWs across the NWAtlantic, LabSea, and EMed. These circulation regimes were associated with persistent anticyclonic anomalies, subsidence, reduced wind speeds and enhanced net heat flux into the ocean, conditions that favored stratification and limited vertical heat redistribution. Earlier MHWs in the NEAtlantic and SubTAtlantic during May–June coincided with NAO^+ and $SCAN^-$ and were further reinforced by a weakened Azores High and anomalously weak trade winds.

To capture these dynamics more comprehensively, we integrated multiple atmospheric variables—including SLP, zg_{500}, wind, T_{max} and ASHF—into our RGCCA framework. This approach allowed us to identify the joint modes of variability that govern regional SSTA. The leading mode explained over 40% of the spatial variance in SSTA and correlated strongly ($r > 0.8$) with predictor time components, confirming the robustness of the circulation linkages. Furthermore, the RGCCA modes aligned with well-established teleconnection indices (NAO, SCAN), lending physical consistency to the statistical results.

Taken together, these findings emphasize that compound atmospheric drivers, particularly the interaction of multiple teleconnection patterns and pressure systems, play a decisive role in the genesis and maintenance of MHWs. As such, efforts to develop MHW early warning systems and attribution frameworks should prioritize real-time monitoring of large-scale atmospheric circulation, particularly during boreal summer when subtropical and extratropical interactions are strongest. The application of RGCCA provides a powerful tool for diagnosing such compound air–sea events and represents a methodological advance for operational forecasting and climate risk assessment under ongoing global warming.

Data availability statement

NOAA OISST v2.1 (1981–present) is available at https://psl.noaa.gov/data/gridded/data.noaa.oisst.v2.highres.html. ERA5 pressure- and single-level reanalyses (1940–present) are at https://cds.climate.copernicus.eu. MHWs were detected with the MATLAB toolbox of Zhao and Marin (2019) (https://github.com/ZijieZhaoMMHW/m_mhw1.0), equivalent to Python/R modules (Hobday *et al* 2016; Schlegel and Smit 2018). RGCCA analyses used the R package of Girka *et al* (2023) (https://github.com/rgcca-factory/RGCCA).

Acknowledgments

Elena Xoplaki and Niklas Luther acknowledge support from the EU Horizon 2020 project CLINT (101003876); Elena Xoplaki and Jürg Luterbacher from the Horizon Europe project MedEWSa (101121192); and Elena Xoplaki and Lorine Behr from the BMBF project ClimXtreme II—CROP4Europe (01LP2324C).

ORCID iDs

Lorine Behr 0000-0002-1069-593X
Elena Xoplaki 0000-0002-2745-2467
Niklas Luther 0000-0002-2019-942X
Simon A Josey 0000-0002-1683-8831
Jürg Luterbacher 0000-0002-8569-0973

References

Androulidakis Y S and Krestenitis Y N 2022 Sea surface temperature variability and marine heat waves over the Aegean, Ionian, and Cretan Seas from 2008–2021 *J. Mar. Sci. Eng.* **10** 42

Barnett T P and Preisendorfer R 1987 Origins and levels of monthly and seasonal forecast skill for United States surface air temperatures determined by canonical correlation analysis *Mon. Weather Rev.* **115** 1825–50

Barnston A G and Livezey R E 1987 Classification, seasonality and persistence of low-frequency atmospheric circulation patterns *Mon. Weather Rev.* **115** 1083–126

Behr L, Luther N, Josey S A, Luterbacher J, Wagner S and Xoplaki E 2022 On the representation of Mediterranean overflow waters in global climate models *J. Phys. Oceanogr.* **52** 1397–413

Bensoussan N, Chiggiato J, Buongiorno Nardelli B, Pisano A and Garrabou J 2019 Insights on 2017 marine heat waves in the Mediterranean Sea. In: Copernicus marine service ocean state report, issue 3 *J. Oper. Oceanogr.* **12** s26–s30

Berthou S *et al* 2024 Exceptional atmospheric conditions in June 2023 generated a northwest European marine heatwave which contributed to breaking land temperature records *Commun. Earth Environ.* **5** 1–11

Bonino G, McAdam R, Athanasiadis P, Cavicchia L, Rodrigues R R, Scoccimarro E, Tibaldi S and Masina S 2025 Mediterranean summer marine heatwaves triggered by weaker winds under subtropical ridges *Nat. Geosci.* (https://doi.org/10.1038/s41561-025-01762-9)

Blunden J and Boyer T 2024 State of the climate in 2023 *Bull. Am. Meteorol. Soc.* **105** S1–484

Bueh C and Nakamura H 2007 Scandinavian pattern and its climatic impact *Q. J. R. Meteorol. Soc.* **133** 2117–31

Capotondi A *et al* 2024 A global overview of marine heatwaves in a changing climate *Commun. Earth Environ.* **5** 1–17

Carroll J D 1968a Equations and tables for a generalization of canonical correlation analysis to three or more sets of variables *Unpublished companion paper to Carroll, J.D. (1968a)*

Carroll J D 1968b Generalization of canonical correlation analysis to three of more sets of variables *Proc. 76th Convention of the American Psychological Association* pp 227–8

Cassou C, Terray L and Phillips A S 2005 Tropical Atlantic influence on European heat waves *J. Clim.* **18** 2805–11

Chafik L, Nilsen J E Ø and Dangendorf S 2017 Impact of North Atlantic teleconnection patterns on Northern European sea level *J. Mar. Sci. Eng.* **5** 43

Chauhan A, Smith P A H, Rodrigues F, Christensen A, John M S and Mariani P 2023 Distribution and impacts of long-lasting marine heat waves on phytoplankton biomass *Front. Mar. Sci.* **10** 1177571

Chen K, Gawarkiewicz G G, Lentz S J and Bane J M 2014 Diagnosing the warming of the Northeastern U.S. Coastal Ocean in 2012: a linkage between the atmospheric jet stream variability and ocean response *J. Geophys. Res. Oceans* **119** 218–27

Cheung W W L and Frölicher T L 2020 Marine heatwaves exacerbate climate change impacts for fisheries in the northeast Pacific *Sci. Rep.* **10** 6678

CMEMS 2023 The 2023 Northern Hemisphere summer marks record-breaking Oceanic events (available at: https://marine.copernicus.eu/news/2023-northern-hemisphere-summer-record-breaking-oceanic-events) (Accessed 13 September 2024)

Diamond M S 2023 Detection of large-scale cloud microphysical changes within a major shipping corridor after implementation of the International Maritime Organization 2020 fuel sulfur regulations *Atmos. Chem. Phys.* **23** 8259–69

Dong T *et al* 2025 Record-breaking 2023 marine heatwaves *Science* **389** 369–74

England M H, Li Z, Huguenin M F, Kiss A E, Sen Gupta A, Holmes R M and Rahmstorf S 2025 Drivers of the extreme North Atlantic marine heatwave during 2023 *Nature* **642** 1–8

Filbee-Dexter K, Wernberg T, Grace S P, Thormar J, Fredriksen S, Narvaez C N, Feehan C J and Norderhaug K M 2020 Marine heatwaves and the collapse of marginal North Atlantic kelp forests *Sci. Rep.* **10** 13388

Folland C K, Knight J, Linderholm H W, Fereday D, Ineson S and Hurrell J W 2009 The summer North Atlantic Oscillation: past, present, and future *J. Clim.* **22** 1082–103

Frölicher T L, Fischer E M and Gruber N 2018 Marine heatwaves under global warming *Nature* **560** 360–4

Garali I *et al* 2018 A strategy for multimodal data integration: application to biomarkers identification in spinocerebellar ataxia *Brief. Bioinform.* **19** 1356–69

Garrabou J *et al* 2009 Mass mortality in Northwestern Mediterranean rocky benthic communities: effects of the 2003 heat wave *Glob. Change Biol.* **15** 1090–103

Garrabou J *et al* 2022 Marine heatwaves drive recurrent mass mortalities in the Mediterranean Sea *Glob. Change Biol.* **28** 5708–25

Girka F, Camenen E, Peltier C, Gloaguen A, Guillemot V, Le Brusquet L and Tenenhaus A 2023 Multiblock data analysis with the RGCCA package *J. Stat. Softw.* 1–36

Goreau T J F and Hayes R L 2024 2023 Record marine heat waves: coral reef bleaching HotSpot maps reveal global sea surface temperature extremes, coral mortality, and ocean circulation changes *Oxford Open Clim. Change* **4** kgae005

Hamdeno M and Alvera-Azcaráte A 2023 Marine heatwaves characteristics in the Mediterranean Sea: case study the 2019 heatwave events *Front. Mar. Sci.* **10** 1093760

Hersbach H *et al* 2020 The ERA5 global reanalysis *Q. J. R. Meteorol. Soc.* **146** 1999–2049

Hobday A J *et al* 2016 A hierarchical approach to defining marine heatwaves *Prog. Oceanogr.* **141** 227–38

Hobday A J *et al* 2018 Categorizing and Naming marine heatwaves *Oceanography* **31** 162–73

Holbrook N J *et al* 2019 A global assessment of marine heatwaves and their drivers *Nat. Commun.* **10** 2624

Huang B, Liu C, Banzon V, Freeman E, Graham G, Hankins B, Smith T and Zhang H-M 2021 Improvements of the daily optimum interpolation sea surface temperature (DOISST) version 2.1 *J. Clim.* **34** 2923–39

Hughes T P *et al* 2018 Global warming transforms coral reef assemblages *Nature* **556** 492–6

Hurrell J W, Kushnir Y, Ottersen G and Visbeck M 2003 An overview of the North Atlantic Oscillation *The North Atlantic Oscillation: Climatic Significance and Environmental Impact* (American Geophysical Union (AGU)) pp 1–35

Ibrahim O, Mohamed B and Nagy H 2021 Spatial variability and trends of marine heat waves in the Eastern Mediterranean Sea over 39 years *J. Mar. Sci. Eng.* **9** 643

Intergovernmental Panel on Climate Change (IPCC), ed 2022 Extremes, abrupt changes and managing risks *The Ocean and Cryosphere in a Changing Climate: Special Report of the Intergovernmental Panel on Climate Change* (Cambridge University Press) pp 589–656

Josey S A and Schroeder K 2011 Impacts of atmospheric modes of variability on Mediterranean Sea surface heat exchange *J. Geophys. Res. Oceans* **116** C02032

Josey S A and Schroeder K 2023 Declining winter heat loss threatens continuing ocean convection at a Mediterranean dense water formation site *Environ. Res. Lett.* **18** 024005

Kornhuber K, Petoukhov V, Karoly D, Petri S, Rahmstorf S and Coumou D 2017 Summertime planetary wave resonance in the Northern and Southern Hemispheres *J. Clim.* **30** 6133–50

Kuhlbrodt T, Swaminathan R, Ceppi P and Wilder T 2024 A glimpse into the future: the 2023 Ocean temperature and sea ice extremes in the context of longer-term climate change *Bull. Am. Math. Soc.* **105** E474–485

Le Grix N, Burger F A and Frölicher T L 2025 Surface and subsurface compound marine heatwave and biogeochemical extremes under climate change *Glob. Biogeochem. Cycles* **39** e2025GB008514

Li K, Zheng F, Zhu J and Zeng Q-C 2024 El Niño and the AMO sparked the astonishingly large margin of warming in the global mean surface temperature in 2023 *Adv. Atmos. Sci.* **41** 1017–22

Marcos M, Amores A, Agulles M, Robson J and Feng X 2025 Global warming drives a threefold increase in persistence and 1 °C rise in intensity of marine heatwaves *Proc. Natl Acad. Sci. USA* **122** e2413505122

Marullo S *et al* 2023 Record-breaking persistence of the 2022/23 marine heatwave in the Mediterranean Sea *Environ. Res. Lett.* **18** 114041

McCarthy G D, Plecha S, Charria G, Simon A, Poppeschi C and Russo A 2023 The marine heatwave west of Ireland in June 2023 *Weather* **78** 321–3

Mills K *et al* 2013 Fisheries management in a changing climate: lessons from the 2012 ocean heat wave in the Northwest Atlantic *Oceanography* **26** 191–5

Miralles D G, Teuling A J, van Heerwaarden C C and Vilà-guerau de Arellano J 2014 Mega-heatwave temperatures due to combined soil desiccation and atmospheric heat accumulation *Nat. Geosci.* **7** 345–9

North G R, Bell T L, Cahalan R F and Moeng F J 1982 Sampling errors in the estimation of empirical orthogonal functions *Mon. Weather Rev.* **110** 699–706

O'Reilly C H, Woollings T and Zanna L 2017 The dynamical influence of the Atlantic Multidecadal oscillation on continental climate *J. Clim.* **30** 7213–30

Pastor F and Khodayar S 2023 Marine heat waves: characterizing a major climate impact in the Mediterranean *Sci. Total Environ.* **861** 160621

Perez E, Ryan S, Andres M, Gawarkiewicz G, Ummenhofer C C, Bane J and Haines S 2021 Understanding physical drivers of the 2015/16 marine heatwaves in the Northwest Atlantic *Sci. Rep.* **11** 17623

Rodríguez-Fonseca B *et al* 2015 Variability and predictability of West African droughts: a review on the role of sea surface temperature anomalies *J. Clim.* **28** 4034–60

Schäfer J and Strimmer K 2005 A shrinkage approach to large-scale covariance matrix estimation and implications for functional genomics *Stat. Appl. Genet. Mol. Biol.* **4**

Schlegel R W and Smit A J 2018 heatwaveR: a central algorithm for the detection of heatwaves and cold-spells *J. Open Source Softw.* **3** 821

Schlegel R W, Oliver E C J and Chen K 2021 Drivers of marine heatwaves in the Northwest Atlantic: the role of air–sea interaction during onset and decline *Front. Mar. Sci.* **8** 627970

Sen Gupta A *et al* 2020 Drivers and impacts of the most extreme marine heatwave events *Sci. Rep.* **10** 19359

Simon A, Pires C, Frölicher T L and Russo A 2023a Long-term warming and interannual variability contributions' to marine heatwaves in the Mediterranean *Weather Clim. Extremes* **42** 100619

Simon A, Pires C, Frölicher T L and Russo A 2023b Coastal and regional marine heatwaves and cold spells in the northeastern Atlantic *Ocean Sci.* **19** 1339–55

Sims L D, Subrahmanyam B and Trott C B 2022 Ocean–atmosphere variability in the Northwest Atlantic Ocean during active marine heatwave years *Remote Sens.* **14** 2913

Smale D A *et al* 2019 Marine heatwaves threaten global biodiversity and the provision of ecosystem services *Nat. Clim. Change* **9** 306–12

Smith K E, Burrows M T, Hobday A J, King N G, Moore P J, Sen Gupta A, Thomsen M S, Wernberg T and Smale D A 2023 Biological impacts of marine heatwaves *Annu. Rev. Mar. Sci.* **15** 119–45

Stefanon M, D'Andrea F and Drobinski P 2012 Heatwave classification over Europe and the Mediterranean region *Environ. Res. Lett.* **7** 014023

Tenenhaus A and Tenenhaus M 2011 Regularized generalized canonical correlation analysis *Psychometrika* **76** 257–84

Tenenhaus M, Tenenhaus A and Groenen P J F 2017 Regularized generalized canonical correlation analysis: a framework for sequential multiblock component methods *Psychometrika* **82** 737–77

Terhaar J, Burger F A, Vogt L, Frölicher T L and Stocker T F 2025 Record sea surface temperature jump in 2023–2024 unlikely but not unexpected *Nature* **639** 942–6

Vogt L, Burger F A, Griffies S M and Frölicher T L 2022 Local drivers of marine heatwaves: a global analysis with an earth system model *Front. Clim.* **4** 847995

Wernberg T 2021 Marine heatwave drives collapse of kelp forests in Western Australia *Ecosystem Collapse and Climate Change* (*Ecological Studies*) vol 241, ed J G Canadell and R B Jackson (Springer International Publishing) pp 325–43

Xoplaki E, González-Rouco J F, Luterbacher J and Wanner H 2003a Mediterranean summer air temperature variability and its connection to the large-scale atmospheric circulation and SSTs *Clim. Dyn.* **20** 723–39

Xoplaki E, González-Rouco J F, Luterbacher J and Wanner H 2003b Interannual summer air temperature variability over Greece and its connection to the large-scale atmospheric circulation and Mediterranean SSTs 1950–1999 *Clim. Dyn.* **20** 537–54

Zhao Z and Marin M 2019 A MATLAB toolbox to detect and analyze marine heatwaves *J. Open Source Softw.* **4** 1124